



**HAL**  
open science

## Opening of mitochondrial permeability transition pore in cardiomyocytes: is ferutinin a suitable tool for its assessment?

Juliette Bréhat, Mathieu Panel, Bijan Ghaleh, Didier Morin

### ► To cite this version:

Juliette Bréhat, Mathieu Panel, Bijan Ghaleh, Didier Morin. Opening of mitochondrial permeability transition pore in cardiomyocytes: is ferutinin a suitable tool for its assessment?. *Fundamental & Clinical Pharmacology*, 2023, 10.1111/fcp.12879 . hal-04067748

**HAL Id: hal-04067748**

**<https://hal.science/hal-04067748>**

Submitted on 13 Apr 2023

**HAL** is a multi-disciplinary open access archive for the deposit and dissemination of scientific research documents, whether they are published or not. The documents may come from teaching and research institutions in France or abroad, or from public or private research centers.

L'archive ouverte pluridisciplinaire **HAL**, est destinée au dépôt et à la diffusion de documents scientifiques de niveau recherche, publiés ou non, émanant des établissements d'enseignement et de recherche français ou étrangers, des laboratoires publics ou privés.

1

2 **Opening of mitochondrial permeability transition pore in cardiomyocytes: is**  
3 **ferutinin a suitable tool for its assessment?**

4

5

6 Juliette Bréhat<sup>1</sup>, Mathieu Panel<sup>1</sup>, Bijan Ghaleh<sup>1</sup>, Didier Morin<sup>1\*</sup>

7

8 <sup>1</sup>INSERM U955-IMRB, team Ghaleh, UPEC, Ecole Nationale Vétérinaire d'Alfort, Créteil,  
9 France.

10

11

12 \*Corresponding author: Didier MORIN, PhD, INSERM U955, Team Ghaleh, Faculté de  
13 Santé, 8 rue du général Sarrail, 94000, Créteil, France, E-mail: [didier.morin@inserm.fr](mailto:didier.morin@inserm.fr)

14

15 **Abstract**

16 Mitochondrial permeability transition pore (mPTP) opening is a critical event leading to cell  
17 injury during myocardial ischemia-reperfusion but having a reliable cellular model to study  
18 the effect of drugs targeting mPTP is an unmet need. This study evaluated whether the Ca<sup>2+</sup>  
19 electrogenic ionophore ferutinin is a relevant tool to induce mPTP in cardiomyocytes. mPTP  
20 opening was monitored using the calcein/cobalt fluorescence technique in adult  
21 cardiomyocytes isolated from wild-type and cyclophilin D (CypD) knock-out mice.  
22 Concomitantly, the effect of ferutinin was assessed in isolated myocardial mitochondria. Our  
23 results confirmed the Ca<sup>2+</sup> ionophoric effect of ferutinin in isolated mitochondria and  
24 cardiomyocytes. Ferutinin induced all the hallmarks of mPTP opening in cells (loss of calcein,  
25 of mitochondrial potential and cell death), but none of them could be inhibited by CypD  
26 deletion or cyclosporine A, indicating that mPTP opening was not the major contributor to the  
27 effect of ferutinin. This was confirmed in isolated mitochondria where ferutinin acts by  
28 different mechanisms dependent and independent of the mitochondrial membrane potential.  
29 At low ferutinin/mitochondria concentration ratio, ferutinin displays protonophoric-like  
30 properties, lowering the mitochondrial membrane potential and limiting oxidative  
31 phosphorylation without mitochondrial swelling. At high ferutinin/mitochondria ratio, ferutinin  
32 induced a sudden Ca<sup>2+</sup> independent mitochondrial swelling, which is only partially inhibited  
33 by cyclosporine A.

34 Together, these result show that ferutinin is not a suitable tool to investigate CypD-  
35 dependent mPTP opening in isolated cardiomyocytes because it possesses other  
36 mitochondrial properties such as swelling induction and mitochondrial uncoupling properties  
37 which impede its utilization.

38

39 **Keywords**

40 Ferutinin; Mitochondria; permeability transition pore; cardiomyocytes.

41

42 **List of abbreviations**

43 CypD: cyclophilin D; mPTP: mitochondrial permeability transition pore; FCCP: carbonyl  
44 cyanide 4-(trifluoromethoxy)phenylhydrazone

45

## 46 **1. Introduction**

47 The mitochondrial permeability transition is a critical event in cell death. It corresponds to an  
48 increase in the permeability of the inner mitochondrial membrane and is mediated by  
49 opening of the permeability transition pore (mPTP). mPTP contributes to cell injuries in a  
50 number of diseases and more particularly during myocardial ischemia–reperfusion [1].  
51 Despite a considerable number of studies, the molecular structure of this channel remains  
52 unknown, potential constitutive proteins having been ruled out by genetic modulation. In  
53 recent years, experimental evidence suggest that ATP synthase participates to the formation  
54 of the pore [2]. However, there is also a common agreement to consider that excess  
55 intramitochondrial  $\text{Ca}^{2+}$  is a crucial factor to trigger mPTP opening [3] and that cyclophilin D  
56 (CypD), a soluble protein located within the mitochondrial matrix, is a key regulator as it  
57 lowers the  $\text{Ca}^{2+}$  threshold triggering mPTP formation [4].

58 The critical role of mPTP opening in cell death suggests that its inhibition may represent an  
59 effective therapeutic approach in several pathological conditions. Therefore, the identification  
60 of novel mPTP inhibitors should be considered with great interest but, currently, a convenient  
61 and reliable cardiomyocyte model is lacking to study potential inhibitors.

62 As  $\text{Ca}^{2+}$  plays a major role in mPTP opening, we previously explored the effect of three  $\text{Ca}^{2+}$   
63 ionophores (A23187, ionomycin, and ETH129) as possible inducers of mPTP opening with  
64 the objective to develop such a model in primary cardiomyocytes where  $\text{Ca}^{2+}$  fluxes have a  
65 fundamental role. We demonstrated that they were not suitable to induce mPTP opening in  
66 adult murine cardiomyocytes because their mechanism of  $\text{Ca}^{2+}$  transport was not effective  
67 enough or they displayed effects independent from mPTP opening [5]. The  $\text{Ca}^{2+}$  ionophore  
68 strategy remains, however, an interesting approach.

69 In the present study, we investigated the effect of ferutinin, jaeschkeanadiol p-  
70 hydroxybenzoate, for its  $\text{Ca}^{2+}$  ionophore properties. Ferutinin was shown to mobilize  $\text{Ca}^{2+}$  in  
71 cells, to increase mitochondrial  $\text{Ca}^{2+}$  permeability and to induce mitochondrial  $\text{Ca}^{2+}$  loading  
72 and depolarization [6]. Opening of the mPTP appeared as a possible mechanism of this  
73 depolarization [7], and several studies demonstrate that ferutinin possesses antiproliferative  
74 effects through the activation of the intrinsic apoptotic pathway and mPTP opening [8-11]. A  
75 recent study also showed that ferutinin induces mPTP opening in liver mitochondria [12].  
76 Unlike A23187 and ionomycin, which equilibrate  $\text{Ca}^{2+}$  concentrations between cell  
77 compartments and the extracellular space in an electroneutral manner, ferutinin is an  
78 electrogenic  $\text{Ca}^{2+}$  ionophore. This mechanism could be more appropriate to promote a  
79 physiological model of mitochondrial  $\text{Ca}^{2+}$  overload [7]. Therefore, using the calcein loading  
80  $\text{CoCl}_2$  quenching technique [13], we investigated the effect of ferutinin on mPTP opening in

81 primary cardiomyocytes isolated from adult mice and we examined its effect on isolated  
82 myocardial mitochondria.

83

## 84 **2. Materials and Methods**

### 85 **2.1. Animals**

86 All animal procedures used in this study were in accordance with the Directives of the  
87 European Parliament (2010/63/EU-848 EEC) and the recommendations of the French  
88 Ministère de l'Agriculture. Male C57BL/6J mice (8 to 10 week-old) were purchased from  
89 Janvier (Le Genest-St-Isle, France). CypD knock-out mice (*Ppif*<sup>-/-</sup> mice) were obtained from  
90 Jackson Laboratories (Bar Harbor, Maine, USA). Mice were housed in an air-conditioned  
91 room with a 12 h light–dark cycle and received standard rodent chow and drinking water *ad*  
92 *libitum*.

### 93 **2.2. Isolation of cardiac mitochondria**

94 Mitochondria were isolated as described previously [14]. Briefly, hearts were scissor minced  
95 and homogenized in a buffer (220 mM mannitol, 70 mM sucrose, 10 mM HEPES, 2 mM  
96 EGTA, pH 7.4 at 4°C) using a Potter-Elvehjem glass homogenizer in a final volume of 10 mL.  
97 The homogenate was filtered and centrifuged at 1000g for 5 min at 4°C. The supernatant  
98 was centrifuged at 10000g for 10 min at 4°C. The mitochondrial pellet was resuspended in  
99 50 µL of homogenization buffer without EGTA and protein concentration was determined  
100 using the advanced protein assay reagent (Sigma catalog number #57697). In experiments  
101 requiring a lot of mitochondria, mitochondrial preparations from two to three hearts were  
102 pooled.

### 103 **2.3. Measurement of mitochondrial respiration**

104 Mitochondrial oxygen consumption was measured at 30°C with a Clark-type electrode  
105 (Hansatech Instruments Ltd, Norfolk, UK). Mitochondria (0.4 mg protein/mL) were incubated  
106 in a respiration buffer containing 100 mM KCl, 50 mM sucrose, 10 mM HEPES and 5 mM  
107 KH<sub>2</sub>PO<sub>4</sub>, pH 7.4 at 30°C. Respiration was initiated by addition of 5 mM glutamate/ 5 mM  
108 malate (state 2, substrate dependent respiration rate). Then, ATP synthesis was induced by  
109 adding 0.4 mM ADP (state 3, ADP-dependent respiration rate, V<sub>3</sub>). The rate of state 4  
110 respiration was measured either after exhaustion of ADP (V<sub>4</sub>) or after addition of 1 µM of  
111 carboxyatractyloside (V<sub>4CAT</sub>) and the respiratory control ratio (state 3/state 4) was evaluated.  
112 When tested, ferutinin was added 1 min after the beginning of state 2 respiration.

### 113 **2.4. Measurement of mitochondrial membrane potential**

114 Mitochondrial membrane potential ( $\Psi$ ) was evaluated by the uptake of the fluorescent dye  
115 rhodamine 123, which accumulates electrophoretically into energized mitochondria in  
116 response to their negative-inner membrane potential. The respiratory substrates

117 glutamate/malate (5/5 mM) and rhodamine 123 (0.2  $\mu$ M) were added to 1 mL of respiration  
118 buffer into the cuvette maintained at 30°C. Fluorescence was monitored over time using a  
119 Perkin-Elmer SA LS 50B fluorescence spectrometer (excitation wavelength = 503 nm,  
120 emission wavelength = 527 nm). After 40 s of initial monitoring, mitochondria (0.2 mg/mL  
121 protein) were added and the effect of ferutinin on membrane potential was examined  
122 following addition of the compound at t = 120-150 s. When used, carboxyatractyloside (1  $\mu$ M)  
123 was added before ferutinin. Carbonyl cyanide-p-trifluoromethoxyphenylhydrazone (FCCP, 1  
124  $\mu$ M) was added to depolarize the mitochondrial membrane potential thus acting as internal  
125 reference.

## 126 **2.5. Mitochondrial swelling assays**

127 Mitochondrial swelling was assessed by measuring the change in absorbance at 540 nm  
128 using a Jasco V-530 spectrophotometer equipped with magnetic stirring and thermostatic  
129 control. Mitochondria energized with glutamate/malate (5 mM each) were incubated 30 s at  
130 30°C in the respiration buffer before the induction of swelling with ferutinin.

131 In de-energized conditions, mitochondria were incubated 30 s at 30°C without substrate in  
132 the respiration buffer including 1  $\mu$ M rotenone and 1  $\mu$ M antimycin at pH 7.4 before inducing  
133 swelling with ferutinin. In both conditions, cyclosporine A (1  $\mu$ M) was introduced at the onset  
134 of the incubation period.

135 In some experiments, respiration buffer was replaced by a sucrose-HEPES buffer containing  
136 250 mM sucrose and 10 mM HEPES at pH 7.4.

137 Swelling experiments were analyzed by measuring the initial rate of swelling which was  
138 expressed as change in absorbance/s.

## 139 **2.6. Measurement of intra-mitochondrial calcium**

140 Intra-mitochondrial  $\text{Ca}^{2+}$  was evaluated in isolated mitochondria using the non-fluorescent  
141 probe Rhod-2/AM, which is converted to fluorescent Rhod-2 via the action of esterases.  
142 Isolated mitochondria ( $\approx$  15 mg/mL) were incubated under stirring with Rhod-2/AM (30  $\mu$ M)  
143 for 30 min at 25°C in 500  $\mu$ L of homogenization buffer devoid of EGTA. The suspension was  
144 then diluted 30-fold with the homogenization buffer at 4°C and after centrifugation (10 min,  
145 10000g) the pellet containing loaded mitochondria was resuspended in 100  $\mu$ L of  
146 homogenization buffer.

147 Rhod-2-loaded mitochondria (0.5 mg/mL) were incubated in the respiration buffer (1 mL)  
148 maintained at 30 °C under constant agitation. Intra-mitochondrial  $\text{Ca}^{2+}$  was monitored over

149 time by following Rhod-2 fluorescence using a Perkin Elmer LS50B spectrofluorometer  
150 (exciting wavelength 552 nm; emission wavelength 581 nm).

151

## 152 **2.7. Measurement of intra-mitochondrial pH**

153 Intra-mitochondrial pH (pHi) was evaluated in isolated mitochondria using the non-  
154 fluorescent probe BCECF-AM, which is converted to fluorescent BCECF via the action of  
155 esterases. Isolated mitochondria (15 mg/mL) were incubated under stirring with BCECF-AM  
156 (30  $\mu$ M) for 30 min at 25°C in the homogenization buffer devoid of EGTA. The suspension  
157 was then diluted 30 fold with the homogenization buffer at 4°C and after centrifugation (10  
158 min, 10000g) the pellet containing loaded mitochondria was resuspended in 100  $\mu$ L of  
159 homogenization buffer.

160 BCECF-loaded mitochondria (0.2 mg/mL) were incubated in the respiration or in the sucrose-  
161 HEPES buffer (1 mL) maintained at 30 °C under constant agitation. Fluorescence was  
162 followed using a temperature-controlled spectrofluorometer (Jasco FP-6300) using an  
163 excitation ratio technique (dual excitation wavelength 439 and 488 nm and fixed emission  
164 wavelength at 525 nm). The signals at 439 and 488 nm correspond to the isosbestic point  
165 and to the maximal sensitivity of the probe, respectively. When used, rotenone (1  $\mu$ M),  
166 antimycin (1  $\mu$ M) and cyclosporine A were introduced at the beginning of the experiment.

## 167 **2.8. Measurement of mitochondrial potassium flux.**

168 Mitochondrial potassium flux was assessed with the fluorescent probe PBFI [15,16]. Isolated  
169 mitochondria ( $\approx$  15 mg/mL) were incubated under stirring with 30  $\mu$ M of the potassium  
170 fluorescent indicator acetoxymethyl ester (PBFI, AM) in 500 $\mu$ L of homogenization buffer  
171 devoid of EGTA for 20 min at 25°C. Before incubation, PBFI-AM was mixed with the nonionic  
172 surfactant pluronic F-127 (2:1 ratio, vol/vol) to improve the aqueous solubility of the probe  
173 and thus its mitochondrial loading. After incubation, the suspension was diluted 30-fold with  
174 the homogenization buffer at 4°C, and after centrifugation (10 min, 10000 g) the pellet  
175 containing loaded mitochondria was resuspended in 100  $\mu$ L of homogenization buffer.

176 PBFI-loaded mitochondria (0.2 mg/mL) were incubated in the respiration buffer (1 mL)  
177 maintained at 30 °C under constant agitation. Fluorescence was followed using a  
178 temperature-controlled spectrofluorometer (Jasco FP-6300) using an excitation ratio  
179 technique (dual excitation wavelength 340 and 380 nm and fixed emission wavelength at 525  
180 nm). The signals at 340 and 380 nm correspond to the maximal sensitivity and to the  
181 isosbestic point of the probe, respectively. When used, rotenone (1  $\mu$ M), antimycin (1  $\mu$ M)  
182 and cyclosporine A (1  $\mu$ M) were added at the beginning of the experiment.

## 183 **2.9. Isolation of primary adult mouse cardiomyocytes**

184 Ventricular cardiomyocytes were isolated from mice by an enzymatic technique. The heart  
185 was retrogradely perfused for 15 min at 37°C with a stock perfusion buffer bubbled with  
186 95%O<sub>2</sub>/5%CO<sub>2</sub> containing 133 mM NaCl, 4.7 mM KCl, 0.6 mM KH<sub>2</sub>PO<sub>4</sub>, 0.6 mM Na<sub>2</sub>HPO<sub>4</sub>,  
187 1.2 mM MgSO<sub>4</sub>, 12 mM NaHCO<sub>3</sub>, 10 mM KHCO<sub>3</sub>, 10 mM HEPES, 30 mM taurine, 0.032 mM  
188 phenol red, 5.5 mM glucose, 10 mM 2,3butanedionemonoxime pH 7.4 to wash out blood.  
189 After 2 min of perfusion, liberase (Blendzyme 10 mg/100 mL, Roche Applied Science,  
190 Mannheim, Germany), trypsin EDTA (14 mg/100 mL) and 12.5 μM Ca<sup>2+</sup> were added to the  
191 buffer. After approximately 8-9 min of perfusion, the heart was placed in the same buffer  
192 containing 10% bovine serum albumin pH 7.4 at 37°C to stop the digestion. Ventricles were  
193 then cut into small fragments and cells isolated by stirring the tissue and successive  
194 aspirations of the fragments through a 10 mL pipette. After 10 min, the supernatant was  
195 removed and the remaining tissue fragments were re-exposed to 10 mL of the same buffer.  
196 Then, the cells were suspended in the same buffer and Ca<sup>2+</sup> was gradually added to 1 mM  
197 into an incubator at 37°C. Finally, the cardiomyocytes were suspended in culture medium  
198 M199 supplemented with 1% Insulin-Transferrin-Selenium. They were seeded on 35 mm  
199 Petri dishes (150000 cells/dish) precoated with 10 μg/mL sterilized laminin and incubated for  
200 90 min before being used.

## 201 **2.10. Measurement of mPTP opening, membrane potential, cell death and** 202 **mitochondrial calcium in cells**

203 mPTP opening was assessed by means of the established loading procedure of the cells  
204 with calcein acetoxymethyl ester (calcein-AM) and CoCl<sub>2</sub> resulting in mitochondrial  
205 localization of calcein fluorescence [13,17]. Cells were loaded with 1 μM calcein-AM for 30  
206 min at 37°C in 2 mL of M199, pH=7.4, supplemented with 1 mM CoCl<sub>2</sub> after 20 min of  
207 incubation.

208 They were then washed free of calcein-AM and CoCl<sub>2</sub> and M199 was replaced by Tyrode's  
209 buffer (NaCl 130 mM; KCl 5 mM; HEPES 10 mM; MgCl<sub>2</sub> 1 mM; CaCl<sub>2</sub> 1.8 mM, pH 7.4 at  
210 37°C). To determine cell death, cells were co-loaded with 1.5 μM propidium iodide, which  
211 permeates only the damaged cells. When the mitochondrial membrane potential was  
212 monitored, cardiomyocytes were loaded with 20 nM tetramethylrhodamine methyl ester  
213 (TMRM) for 30 min at 37°C and then rinsed with Tyrode's solution. To monitor mitochondrial  
214 Ca<sup>2+</sup>, cardiomyocytes were loaded with 1.5 μM Rhod-2 AM (ThermoFisher Scientific, Villebon-  
215 sur-Yvette, France) for 30 min at 37°C and then washed free of Rhod-2/AM.

216 The cardiomyocytes were placed into a thermostated (37°C) chamber (Warner Instruments  
217 Inc, Connecticut, USA) which was mounted on the stage of a IX81 Olympus motorized

218 inverted microscope, were perfused with Tyrode's solution at a rate of 0.5 ml/min and were  
219 paced to beat by field stimulation (5 ms, 0.5 Hz).

220 Cardiomyocytes were imaged with the microscope equipped with a mercury lamp as a  
221 source of light for epifluorescence illumination and with a cooled CCD Hamamatsu ORCA  
222 ER digital camera. For detection of calcein fluorescence a 460- to 490nm excitation and a  
223 510 nm emission filters were used. Propidium iodide and TMRM fluorescence were excited  
224 at 520-550 nm and recorded at 580 nm. For the detection of Rhod-2 a 525- to 550nm  
225 excitation and a 580- to 635nm emission filter were used. Images were acquired every 30 or  
226 60 s within the first 30 min and then every 5 min after an illumination time of 25 ms (calcein)  
227 and 70 msec (propidium iodide, TMRM and Rhod-2). Images were analyzed using a digital  
228 epifluorescence imaging software (XCellence, Olympus, Rungis, France).

229 First, for each experiment, the change of fluorescence was observed from a single  
230 cardiomyocyte. Fluorescence was integrated over a region of interest ( $\approx 80 \mu\text{m}^2$ ) and a  
231 fluorescence background corresponding to an area without cells was subtracted. Then, the  
232 global response was analysed by averaging the fluorescence changes obtained from all the  
233 cardiomyocytes (20-30 cells) contained in a single field. For comparative purposes, the  
234 fluorescence intensity minus background was normalized according to the maximal  
235 fluorescence value (initial value for calcein, TMRM, and Rhod-2, final value for propidium  
236 iodide). The time necessary to induce a 50% decrease in calcein fluorescence ([Tcalcein50])  
237 and to induce a 50% increase in propidium iodide fluorescence (time to 50% cell death [Tcell  
238 death50]) were determined.

### 239 **2.11. Statistical analysis**

240 Statistical analysis was performed with GraphPad Prism 9.1.2 (Graph Pad Software, USA).  
241 Data were presented as the means  $\pm$  standard error of mean (SEM). Statistical significance  
242 of differences between two groups was determined using an unpaired two-tailed *t*-test.  
243 Significant differences between more than two groups were evaluated by one-way analysis  
244 of variance (ANOVA) analysis followed by a Tukey's post test if ANOVA produced a  
245 significant value of *F* ( $p < 0.05$ ). Statistical parameters and significance are reported in the  
246 figures and the figure legends.

247

## 248 **3. Results**

### 249 **3.1. Ferutinin displays calcium ionophoretic properties**

250 First, we verified the  $\text{Ca}^{2+}$  ionophoretic properties of ferutinin in isolated cardiac mitochondria.  
251 Fresh isolated mitochondria were loaded with the  $\text{Ca}^{2+}$  sensitive fluorescent dye Rhod-2 as  
252 its acetoxymethyl esters Rhod-2/AM. Rhod-2/AM is hydrolyzed by mitochondrial esterase  
253 and Rhod-2 is entrapped in the mitochondrial matrix space as reported for others  
254 acetoxymethyl ester dyes [18,19]. This allows the monitoring of mitochondrial free  $\text{Ca}^{2+}$   
255 concentration. When mitochondria were energized by the addition of respiratory substrates  
256 (pyruvate/malate), the addition of  $\text{Ca}^{2+}$  in the medium induced a rapid and concentration  
257 dependent increase in fluorescence. This effect was strongly inhibited by the presence of the  
258  $\text{Ca}^{2+}$  uniporter blocker ruthenium red, demonstrating the validity of the method (Fig. 1A).  
259 Then, cardiac mitochondria were incubated in the same buffer in the presence of rotenone  
260 and antimycin to inhibit respiration and therefore the uniporter complex dependent  $\text{Ca}^{2+}$   
261 influx. In these deenergized conditions, ferutinin caused a concentration-dependent  $\text{Ca}^{2+}$   
262 entry into mitochondria, which was not inhibited by ruthenium red confirming the ionophoretic  
263 properties of the drug (Fig 1B). On the contrary, ruthenium red stimulates mitochondrial  $\text{Ca}^{2+}$   
264 uptake, which may be due to the blockade of the uniporter complex avoiding a  $\text{Ca}^{2+}$  efflux  
265 [20]

266 Then we verified the ability of ferutinin to cause mitochondrial  $\text{Ca}^{2+}$  influx in isolated  
267 cardiomyocytes. Mitochondrial compartment of cardiomyocytes were loaded with  $1.5\mu\text{M}$   
268 Rhod-2/AM and then supplemented with increasing concentrations of ferutinin. Ferutinin  
269 induced a time-dependent increase in mitochondrial  $\text{Ca}^{2+}$  confirming the ionophoretic  
270 properties of the drug (Fig 1C).

### 271 **3.2. Ferutinin and mPTP opening in isolated adult cardiomyocytes.**

272 We next investigated the ability of ferutinin to induce mPTP opening in isolated mouse adult  
273 cardiomyocytes. Cells were coloaded with calcein in the presence of  $\text{CoCl}_2$  and TMRM to  
274 monitor mPTP opening and mitochondrial potential, respectively. Figure 2A shows that the  
275 addition of  $25\mu\text{M}$  ferutinin decreased both calcein and TMRM fluorescence concomitantly in  
276 a time-dependent manner, which may be the signs of mPTP opening. Next, we verify if the  
277 mitochondrial calcein loss induced by ferutinin was associated with cell death. We coloaded  
278 mitochondria with calcein/ $\text{CoCl}_2$  and propidium iodide before adding ferutinin. As shown in  
279 Figures 2B and 2C, the decrease in calcein fluorescence was associated with an increase in  
280 propidium iodide fluorescence and these effects were concentration-dependent. At  $5\mu\text{M}$ , the  
281 effect of ferutinin was weak: The loss of calcein fluorescence and cell death were only partial  
282 at 60 min.

283 To confirm the occurrence of mPTP opening in the effect of ferutinin, similar experiments  
284 were performed on cardiomyocytes isolated from CypD knock-out mice which are protected

285 from mPTP opening [21]. CypD deletion slightly delayed both the loss of calcein and the  
286 increase in propidium iodide fluorescence but after 25 min, all the cells lost their calcein and  
287 died (Figures 3A and 3B). Similar results were found at a lower concentration of ferutinin and  
288 in the presence of cyclosporine A, a well-known de-sensitizer of mPTP opening (Figure 3C).  
289 It should be noted that the times necessary to induce a 50 % decrease in calcein ( $T_{\text{calcein}50}$ )  
290 and a 50 % increase in cell death ( $T_{\text{cell death}50}$ ) were not statistically different (Figure 3D). This  
291 suggests that mPTP opening is not the major contributor to the effect of ferutinin and that  
292 other mechanisms contribute to mitochondrial calcein loss, mitochondrial membrane  
293 potential disruption, and cell death in cardiomyocytes. To decipher these mechanisms, we  
294 next investigated isolated cardiac mitochondria.

### 295 **3.3. Ferutinin and mPTP opening in cardiac mitochondria isolated from mice.**

296 To investigate the effect of ferutinin on mPTP opening we examined whether ferutinin could  
297 induce mitochondrial swelling. As depicted in Figure 4A, ferutinin induced a concentration-  
298 dependent swelling in mitochondria energized with glutamate/malate as attested by the  
299 decrease in absorbance of the mitochondrial suspension. The swelling is strongly dependent  
300 on the ferutinin/mitochondria concentration ratio. Under 80 nmol ferutinin/mg mitochondrial  
301 protein, no swelling could be detected. For example, 25  $\mu\text{M}$  ferutinin did not induce swelling  
302 at a mitochondrial protein concentration of 0.4 mg/mL (Figure 4A).

303 Cyclosporine A prevented the swelling induced by ferutinin, highlighting the role of the mPTP  
304 in the swelling process but the inhibition was only partial (Figure 4B) implying the intervention  
305 of other mechanism(s). Surprisingly, the swelling was obtained without  $\text{Ca}^{2+}$  addition, a  
306 critical factor for mPTP opening. Drugs acting on  $\text{Ca}^{2+}$  such as the  $\text{Ca}^{2+}$  chelator EGTA or the  
307 mitochondrial  $\text{Ca}^{2+}$  uniport ruthenium red had no effect on the swelling (Figure S1). This  
308 indicates that part of the swelling of the organelles is due to the formation of a nonspecific  
309 cyclosporine A insensitive permeability of the inner membrane.

310 Similar swelling induction and cyclosporine A inhibition were observed under de-energized  
311 conditions, that is, in the absence of substrate and in the presence of rotenone and antimycin  
312 that fully block the respiratory chain (Figure 4C). This confirms the non-necessity of  $\text{Ca}^{2+}$  and  
313 indicates that mitochondrial membrane potential does not play any role in the swelling  
314 induced by ferutinin. Similarly, the absence of phosphate in the incubation medium (not  
315 shown) did not alter the swelling whereas the utilization of a minimal sucrose-hepes buffer  
316 (devoid of potassium) slowed down the rate of the swelling suggesting the involvement of  
317 potassium in the kinetic of the swelling process (Figure 4C).

### 318 **3.4. Ferutinin inhibits oxidative phosphorylation and mitochondrial membrane potential**

319 To further understand the mechanism by which ferutinin alters mitochondrial function, we  
320 studied the effect of increasing concentration of ferutinin on the rate of oxygen consumption  
321 in myocardial mitochondria energized with glutamate/malate. Ferutinin increased state 4 and  
322 decreased state 3 respiration rate, resulting in a total inhibition of the respiratory coefficient  
323 ratio at 25  $\mu\text{M}$  ferutinin (Figure 5A). This effect was significant even at low  $\mu\text{M}$   
324 concentrations. It was independent from mPTP opening as cyclosporine A was devoid of  
325 effect and the concentrations of ferutinin tested (6.25-25  $\mu\text{M}$ ) did not induce mitochondrial  
326 swelling at 0.4 mg/mL of proteins (Figure 4A). It should be noted that a clear difference was  
327 observed when state 4 respiration value was measured either after exhaustion of ADP ( $V_4$ )  
328 or by addition of carboxyatractyloside ( $V_{4\text{CAT}}$ ). Carboxyatractyloside limited the increase in  
329  $V_4$  value and thus the decrease in respiratory control ratio. The effect of carboxyatractyloside  
330 is clearly observed in figure 5B showing the basal rate of oxygen consumption by  
331 mitochondria energized with glutamate/malate. Whether introduced before or after ferutinin,  
332 carboxyatractyloside inhibited oxygen consumption induced by ferutinin.

333 Ferutinin stimulation of respiration was associated with a concentration-dependent decrease  
334 in the membrane potential monitored by the mitochondrial release of rhodamine 123 (Figure  
335 5C). This effect was not altered in the presence of cyclosporine A (Figure S2) and was  
336 obtained in a  $\text{Ca}^{2+}$ -free medium, ruling out the roles of mPTP and of a  $\text{Ca}^{2+}$  ionophoretic  
337 property of the drug in this effect. Ferutinin behaved like the uncoupling agent carbonyl  
338 cyanide 4-(trifluoromethoxy)phenylhydrazone (FCCP), a protonophore which enters  
339 mitochondria in the protonated form, discharging the pH gradient and destroying the  
340 membrane potential. Here again, carboxyatractyloside modulated the effect of ferutinin as it  
341 limited the release of rhodamine 123 at low ferutinin concentrations (Figure 5D).

### 342 **3.5. Ferutinin modulates mitochondrial matrix pH.**

343 To verify a potential protonophore effect of ferutinin, we studied its effect on matrix pH ( $\text{pHi}$ )  
344 using the BCECF method. This represents an interesting approach to study uncoupling  
345 agents as most of them recycle protons across mitochondrial inner membranes, disrupting  
346 proton gradient and decreasing  $\text{pHi}$ . As shown in Figure 6A, feeding the electron transport  
347 chain via complex I with glutamate/malate increased  $\text{pHi}$  as the electron transport chain  
348 extruded protons. The complex I inhibitor rotenone and FCCP abolished the gradient of  
349 protons and thus decreased  $\text{pHi}$  confirming the relevance of this method.

350 Addition of low ferutinin concentrations (6.25 and 12.5  $\mu\text{M}$ ) were also followed by a slow  
351 matrix acidification confirming the protonophoric-like effect of the drug (Figure 6B). At higher  
352 concentrations, ferutinin, unlike FCCP, increased  $\text{pHi}$  with a marked effect at 50  $\mu\text{M}$  (Figure  
353 6B). This increase in  $\text{pHi}$  persisted under de-energized conditions, and was concentration

354 dependent (Figure 6C) but was not observed when a minimal sucrose-hepes buffer devoid of  
355 potassium, which maintains an acidic matrix pH, was used (Figure 6D). In this minimal buffer,  
356 ferutinin induced alkalinization was partially restored by the selective addition of cations  
357 including Na<sup>+</sup> or K<sup>+</sup> in the medium (Figure 6D). This is in accordance with previous data  
358 showing that the acidic matrix pH maintained by nonrespiring mitochondria in sucrose can be  
359 raised by the mitochondrial uptake of cations counteracting the pH-driven proton diffusion  
360 potential [22]. Interestingly, cyclosporine A slightly inhibited the rate of alkalinization of the  
361 mitochondrial matrix induced by high ferutinin concentrations, suggesting the contribution of  
362 mPTP opening in this effect (Figure 6D).

### 363 **3.6. Ferutinin induces potassium transport**

364 As potassium influenced the effect of ferutinin on mitochondrial swelling and pHi, we  
365 measured changes in matrix potassium by loading mitochondria with the potassium selective  
366 probe PBFI. Energization of mitochondria with glutamate/malate generates the electrical  
367 membrane potential, which drives mitochondrial potassium influx [23] (Figure 7A). In these  
368 conditions, addition of low ferutinin concentrations (6.25-25μM) was without effect (Figure  
369 7A). Deenergized conditions, however, revealed a marked uptake of potassium into  
370 mitochondria elicited by the same concentrations of ferutinin (6.25-25μM). This effect is  
371 probably masked in energized conditions because PBFI is saturated by the entry of  
372 potassium generated by the membrane potential. Indeed, determination of mitochondrial  
373 potassium with PBFI exhibits a limited resolution for increases in matrix mitochondria  
374 because the mitochondrial concentration of potassium is high (≈ 150 mM) and PBFI displays  
375 a lower Kd value [16]. Thus, any increase in mitochondrial PBFI fluorescence can only be  
376 relatively small. By contrast, high ferutinin concentrations (> 25μM) elicited a release of  
377 potassium from mitochondria whatever the experimental conditions. The rate of this release  
378 was slow down by cyclosporine A without reduction of the extent of the release (Figure 7B).

379

## 380 **4. Discussion**

381 It is now well-established that mPTP opening plays a key role in numerous diseases [24].  
382 Thus mPTP inhibition possesses a high therapeutic potential but the identification of novel  
383 inhibitors is limited by the undefined molecular identity of the pore and by the lack of cellular  
384 models able to evaluate the effect of the inhibitors. Although it is easy to monitor mPTP  
385 opening in isolated mitochondria, the evaluation of mPTP opening in cells is more complex  
386 since it is regulated by many factors. The development of the calcein loading CoCl<sub>2</sub>  
387 quenching technique was an important step, allowing to investigate the regulation of the pore  
388 and to examine mPTP opening in living cells [25]. However, we currently do not have an

389 easy-to-use tool to induce mPTP in primary cardiomyocytes and to identify potential mPTP  
390 inhibitors, which is an important step to develop cardioprotective agents. In a previous work,  
391 we demonstrated that three  $\text{Ca}^{2+}$  ionophores, which were used to trigger mPTP opening in  
392 different cell types, were not effective in primary cardiomyocytes [5]. The only experimental  
393 protocol we found suitable to induce mPTP opening in primary cardiomyocytes is a model of  
394 hypoxia-reoxygenation [5,26-28]. However, this model involves a complex and long protocol,  
395 which is inappropriate to easily screen and identify novel mPTP inhibitors.

396 Here, we examined the effect of ferutinin because this drug demonstrated  $\text{Ca}^{2+}$  ionophoretic  
397 properties and was able to induce apoptosis in cell lines. Furthermore, it was suggested to  
398 trigger mitochondrial  $\text{Ca}^{2+}$  overload and mPTP opening [7,12]. Using Rhod-2, we confirmed  
399 the  $\text{Ca}^{2+}$  ionophoretic effect of ferutinin since it induced a rapid elevation of matrix  $\text{Ca}^{2+}$  in  
400 isolated cardiac mitochondria and cardiomyocytes. This is in line with the data observed in  
401 Jurkat T-cells where ferutinin mobilized  $\text{Ca}^{2+}$  by both mechanisms, a release of  $\text{Ca}^{2+}$  from  
402 intracellular stores and a cellular entry of extracellular  $\text{Ca}^{2+}$ [8].

403 To assess whether ferutinin could represent an interesting tool to monitor mPTP opening in  
404 cardiomyocytes, we used freshly isolated murine adult cardiomyocytes, which represent a  
405 more physiological setting than cultured cells because they are fully differentiated and can be  
406 electrically paced. Using a direct measurement of mPTP opening by mean of the  
407 calcein/cobalt protocol, we observed a rapid and large calcein loss in cardiomyocytes  
408 challenged with increasing concentrations of ferutinin. Cyclosporine A and CypD deletion  
409 slightly delayed but did not prevent the loss of calcein and the associated cell death,  
410 indicating that mitochondrial depolarization and cell death is not only related to a CypD-  
411 related pore.

412 This is confirmed by the experiments performed in isolated myocardial mitochondria. The  
413 effect of ferutinin is more complex than a sole  $\text{Ca}^{2+}$  ionophore effect since it is able to induce  
414 mitochondrial swelling and depolarization in a free  $\text{Ca}^{2+}$  medium. Ferutinin acts by different  
415 mechanisms at mitochondrial level, dependent and independent of the mitochondrial  
416 membrane potential. At low ferutinin/mitochondria ratio, ferutinin displays protonophoric-like  
417 properties, lowering the mitochondrial membrane potential and limiting oxidative  
418 phosphorylation without mitochondrial swelling. Both parameters were partially restored by  
419 carboxyatractyloside suggesting the involvement of the adenine nucleotide translocase in the  
420 effect of ferutinin. Ferutinin may act on adenine nucleotide translocase to transfer proton  
421 inside mitochondria and the adenine nucleotide translocase blocking effect of  
422 carboxyatractyloside would inhibit the depolarizing effect of ferutinin. This is in line with old but

423 also recent observations that adenine nucleotide translocase can mediate proton transport  
424 across the inner mitochondrial membrane [29,30].

425 The impairment of mitochondrial potential by ferutinin may also reflect the movement of  
426 potassium across the mitochondrial inner membrane since we showed that low ferutinin  
427 concentrations induced a potassium influx into mitochondria. This is compatible with the  
428 ionophoric properties of ferutinin, which is not uniquely selective for  $\text{Ca}^{2+}$  but is able to  
429 increase, to a lesser extent, the permeability of mitochondrial membrane to monovalent  
430 cations [6,31].

431 At high ferutinin/mitochondria concentration ratio, ferutinin induced a sudden mitochondrial  
432 swelling, which is independent of mitochondrial membrane potential. This swelling is inhibited  
433 by cyclosporine A and is accelerated by the presence of potassium in the extramitochondrial  
434 medium. This is indicator of the participation of mPTP opening [1]. However, the mechanism  
435 by which ferutinin induces mPTP opening is different to those described so far since it occurs  
436 in absence of elevated intramitochondrial  $\text{Ca}^{2+}$  concentration and of other factors that  
437 modulate its sensitivity such as oxidative stress or phosphate concentrations. In addition,  
438 cyclosporine A inhibition is only partial and extramitochondrial potassium is not essential,  
439 indicating the contribution of an additional mechanism.

440 The suddenness of the swelling, which is accompanied by a release of potassium in the  
441 extramitochondrial medium and a concomitant complete inhibition of mitochondrial function  
442 suggest that starting at a certain ferutinin/mitochondria concentration ratio, the interaction of  
443 ferutinin with the mitochondrial membrane might alter the topology of the membrane. This  
444 effect could reflect a structural reorganization of the mitochondrial inner membrane induced  
445 by the ferutinin-mediated increase in membrane permeability. This is in line with the results  
446 of Gao et al [10] showing that at high concentrations ferutinin is able to permeabilize the  
447 membrane of red blood cell ghosts in a way similar to digitonin. This mechanism will require  
448 further investigation.

449

450 **5. Conclusion**

451 In conclusion, this study shows that ferutinin is not a suitable tool to assess mPTP opening in  
452 our model of isolated cardiomyocytes. The direct measurement of mPTP opening by means  
453 of the calcein/cobalt protocol demonstrates that this is not the predominant factor leading to  
454 the depolarization of mitochondria and to cell death at the concentrations of ferutinin.  
455 Ferutinin possesses other mitochondrial properties such as induction of swelling and  
456 mitochondrial uncoupling properties. These findings impede its utilization for investigating  
457 mPTP opening in isolated cardiomyocytes.

458

459 **Declaration of competing interest**

460 The authors declare no conflict of interest.

461

462 **Acknowledgements**

463 Juliette Bréhat and Mathieu Panel were supported by doctoral grants (grants number 2018-  
464 057 and 2014-140, respectively) from the Ministère de l'enseignement Supérieur, de la  
465 Recherche et de l'Innovation.

466

467 **References**

- 468 [1] Halestrap AP. A pore way to die: the role of mitochondria in reperfusion injury and  
469 cardioprotection. *Biochem Soc Trans.* 2010;38:841-860.
- 470 [2] Bonora M, Giorgi C, Pinton P. Molecular mechanisms and consequences of mitochondrial  
471 permeability transition. *Nat Rev Mol Cell Biol.* 2022;23:266-285. doi: 10.1038/s41580-021-  
472 00433-y.
- 473 [3] Haworth, R. A. & Hunter, D. R. The Ca<sup>2+</sup> -induced membrane transition in mitochondria.  
474 II. Nature of the Ca<sup>2+</sup> trigger site. *Arch Biochem Biophys.* 1979;195: 460–467.
- 475 [4] Javadov S, Jang S, Parodi-Rullán R, Khuchua Z, Kuznetsov AV. Mitochondrial  
476 permeability transition in cardiac ischemia-reperfusion: whether cyclophilin D is a viable  
477 target for cardioprotection? *Cell Mol Life Sci.* 2017;74:2795-2813. doi: 10.1007/s00018-017-  
478 2502-4.
- 479 [5] Panel M, Ghaleh B, Morin D. Ca<sup>2+</sup> ionophores are not suitable for inducing mPTP  
480 opening in murine isolated adult cardiac myocytes. *Sci Rep.* 2017;7:4283. doi:  
481 10.1038/s41598-017-04618-4.
- 482 [6] Abramov AY, Zamaraeva MV, Hagelgans AI, Azimov RR, Krasilnikov OV. Influence of  
483 plant terpenoids on the permeability of mitochondria and lipid bilayers. *Biochim Biophys Acta.*  
484 2001;1512:98-110. doi: 10.1016/s0005-2736(01)00307-8.
- 485 [7] Abramov AY, Duchen MR. Actions of ionomycin, 4-BrA23187 and a novel electrogenic  
486 Ca<sup>2+</sup> ionophore on mitochondria in intact cells. *Cell Calcium.* 2003;33:101-12. doi:  
487 10.1016/s0143-4160(02)00203-8.
- 488 [8] Macho A, Blanco-Molina M, Spagliardi P et al. Calcium ionophoretic and apoptotic effects  
489 of ferutinin in the human Jurkat T-cell line. *Biochem Pharmacol.* 2004;68:875-63. doi:  
490 10.1016/j.bcp.2004.05.016.
- 491 [9] Poli F, Appendino G, Sacchetti G, Ballero M, Maggiano N, Ranelletti FO. Antiproliferative  
492 effects of daucane esters from *Ferula communis* and *F. arrigonii* on human colon cancer cell  
493 lines. *Phytother Res.* 2005;19:152-7. doi: 10.1002/ptr.1443.
- 494 [10] Gao M, Wong SY, Lau PM, Kong SK. Ferutinin induces in vitro eryptosis/erythroptosis in  
495 human erythrocytes through membrane permeabilization and calcium influx. *Chem Res*  
496 *Toxicol.* 2013;26:1218-28. doi: 10.1021/tx400127w.

- 497 [11] Naji Reyhani Garmroudi S, Karimi E, Oskoueian E, Homayouni-Tabrizi M, Iranshahi M.  
498 Ferutinin: A phytoestrogen from ferula and its anticancer, antioxidant, and toxicity properties.  
499 *J Biochem Mol Toxicol*. 2021;35:e22713. doi: 10.1002/jbt.22713.
- 500 [12] Ilyich T, Charishnikova O, Sekowski S et al. Ferutinin Induces Membrane Depolarization,  
501 Permeability Transition Pore Formation, and Respiration Uncoupling in Isolated Rat Liver  
502 Mitochondria by Stimulation of Ca<sup>2+</sup>-Permeability. *J Membr Biol*. 2018;251:563-572. doi:  
503 10.1007/s00232-018-0032-0.
- 504 [13] Petronilli V, Miotto G, Canton M et al. Transient and long-lasting openings of the  
505 mitochondrial permeability transition pore can be monitored directly in intact cells by changes  
506 in mitochondrial calcein fluorescence. *Biophys J*. 1999;76:725-734. doi: 10.1016/S0006-  
507 3495(99)77239-5.
- 508 [14] Laure L, Long R, Lizano P et al. Cardiac H11 kinase/Hsp22 stimulates oxidative  
509 phosphorylation and modulates mitochondrial reactive oxygen species production:  
510 Involvement of a nitric oxide-dependent mechanism. *Free Radic Biol Med*. 2012;52:2168-76.  
511 doi: 10.1016/j.freeradbiomed.2012.03.001.
- 512 [15] Jezek P, Mahdi F, Garlid KD. Reconstitution of the beef heart and rat liver mitochondrial  
513 K<sup>+</sup>/H<sup>+</sup> (Na<sup>+</sup>/H<sup>+</sup>) antiporter. Quantitation of K<sup>+</sup> transport with the novel fluorescent probe,  
514 PBFI. *J Biol Chem*. 1990;265:10522-6. PMID: 2162352.
- 515 [16] Costa AD, Quinlan CL, Andrukhiv A, West IC, Jabůrek M, Garlid KD. The direct  
516 physiological effects of mitoK(ATP) opening on heart mitochondria. *Am J Physiol Heart Circ*  
517 *Physiol*. 2006;290:H406-15. doi: 10.1152/ajpheart.00794.2005.
- 518 [17] Katoh H, Nishigaki N and Hayashi H. Diazoxide opens the mitochondrial permeability  
519 transition pore and alters Ca<sup>2+</sup> transients in rat ventricular myocytes. *Circulation*  
520 2002;105:2666-2671. doi: 10.1161/01.cir.0000016831.41648.04.
- 521 [18] Lukács GL, Kapus A Measurement of the matrix free Ca<sup>2+</sup> concentration in heart  
522 mitochondria by entrapped fura-2 and quin2. *Biochem J*. 1987;248:609-13. doi:  
523 10.1042/bj2480609.
- 524 [19] Long R, Salouage I, Berdeaux A, Motterlini R, Morin D. CORM-3, a water soluble CO-  
525 releasing molecule, uncouples mitochondrial respiration via interaction with the phosphate  
526 carrier. *Biochim Biophys Acta*. 2014;1837:201-9. doi: 10.1016/j.bbabbio.2013.10.002.
- 527 [20] Jurkowitz MS, Geisbuhler T, Jung DW, Brierley GP. Ruthenium red-sensitive and -  
528 insensitive release of Ca<sup>2+</sup> from uncoupled heart mitochondria. *Arch Biochem Biophys*.  
529 1983;223:120-128. doi:10.1016/0003-9861(83)90577-5

530 [21] Baines CP, Kaiser RA, Purcell NH, et al. Loss of cyclophilin D reveals a critical role for  
531 mitochondrial permeability transition in cell death. *Nature*. 2005;434:658-662.  
532 doi:10.1038/nature03434.

533 [22] Bernardi P, Azzone GF. delta pH induced calcium fluxes in rat liver mitochondria. *Eur J*  
534 *Biochem*. 1979;102:555-62. doi: 10.1111/j.1432-1033.1979.tb04272.x.

535 [23] Garlid KD, Paucek P. Mitochondrial potassium transport: the K(+) cycle. *Biochim*  
536 *Biophys Acta*. 2003;1606:23-41. doi: 10.1016/s0005-2728(03)00108-7

537 [24] Boyenle ID, Oyedele AK, Ogunlana AT et al. Targeting the mitochondrial permeability  
538 transition pore for drug discovery: Challenges and opportunities. *Mitochondrion*. 2022;63:57-  
539 71. doi: 10.1016/j.mito.2022.01.006.

540 [25] Bonora M, Morganti C, Morciano G, Giorgi C, Wieckowski MR, Pinton P. Comprehensive  
541 analysis of mitochondrial permeability transition pore activity in living cells using  
542 fluorescence-imaging-based techniques. *Nat Protoc*. 2016;11:1067-80. doi:  
543 10.1038/nprot.2016.064.

544 [26] Obame FN, Plin-Mercier C, Assaly R et al. Cardioprotective effect of morphine and a  
545 blocker of glycogen synthase kinase 3 beta, SB216763 [3-(2,4-dichlorophenyl)-4(1-methyl-  
546 1H-indol-3-yl)-1H-pyrrole-2,5-dione], via inhibition of the mitochondrial permeability transition  
547 pore. *J Pharmacol Exp Ther*. 2008;326:252-8. doi: 10.1124/jpet.108.138008.

548 [27] Schaller S, Paradis S, Ngoh GA et al. TRO40303, a new cardioprotective compound,  
549 inhibits mitochondrial permeability transition. *J Pharmacol Exp Ther*. 2010;333:696-706. doi:  
550 10.1124/jpet.110.167486.

551 [28] Hansson MJ, Llwyd O, Morin D et al. Differences in the profile of protection afforded by  
552 TRO40303 and mild hypothermia in models of cardiac ischemia/reperfusion injury. *Eur J*  
553 *Pharmacol*. 2015;760:7-19. doi: 10.1016/j.ejphar.2015.04.009

554 [29] Panov A, Filippova S, Lyakhovich V. Adenine nucleotide translocase as a site of  
555 regulation by ADP of the rat liver mitochondria permeability to H<sup>+</sup> and K<sup>+</sup> ions. *Arch Biochem*  
556 *Biophys*. 1980;199:420-6. doi: 10.1016/0003-9861(80)90298-2.

557 [30] Bertholet AM, Chouchani ET, Kazak L et al. H<sup>+</sup> transport is an integral function of the  
558 mitochondrial ADP/ATP carrier. *Nature*. 2019;571:515-520. doi: 10.1038/s41586-019-1400-3.

559 [31] Zamaraeva MV, Hagelgans AI, Abramov AY et al. Ionophoretic properties of ferutinin.  
560 *Cell Calcium*. 1997;22:235-41. doi: 10.1016/s0143-4160(97)90062-2.

561

562 **Legends for Figures**

563

564 **Figure 1:** Ferutinin induces mitochondrial  $\text{Ca}^{2+}$  uptake in isolated mouse mitochondria and  
565 cardiomyocytes.

566  $\text{Ca}^{2+}$  uptake was assessed by measuring the change in fluorescence in mitochondria and  
567 cardiomyocytes preloaded with Rhod-2.

568 **A:** Representative experiment showing mitochondrial uptake of increasing concentrations of  
569  $\text{Ca}^{2+}$  in the absence or in the presence of 5  $\mu\text{M}$  ruthenium red (RR). Mitochondria (0.4 mg/mL)  
570 were incubated in a respiration buffer and energized with glutamate/malate (G/M). Then  
571 increasing concentrations of  $\text{Ca}^{2+}$  (40, 60 and 100  $\mu\text{M}$ ) were added in the absence or in the  
572 presence of RR.

573 **B:** Representative experiment showing the effect of ferutinin in deenergized mitochondria.  
574 Mitochondria (0.4mg/mL) were incubated in the presence of rotenone. At  $t=25$  s, 60  $\mu\text{M}$   $\text{Ca}^{2+}$   
575 were added. Then, increasing concentrations of ferutinin (FE) 25, 50 and 75  $\mu\text{M}$  were added  
576 in the absence or in the presence of RR.

577 **C:** Rhod2-loaded cardiomyocytes were incubated in Tyrode's buffer for 4 min and then ferutinin  
578 was added. Fluorescence values were obtained by averaging pixel intensities after background  
579 subtraction in an area containing 25-30 cells and were normalized as a percentage of the  
580 initial value. Each trace represents the mean  $\pm$  SEM of four to seven experiments. The ordinate  
581 of the bar graph is the value of Rhod-2 fluorescence observed at 12 min in the figure.  $p<0.05$   
582 versus 0 and 5  $\mu\text{M}$  ferutinin.

583 AU: arbitrary units.

584

585 **Figure 2:** Effect of ferutinin on mitochondrial calcein, TMRM and propidium iodide (PI)  
586 fluorescence in isolated adult cardiomyocytes.

587 Isolated adult cardiomyocytes were incubated in Tyrode's buffer at 37 °C and co-loaded with  
588 calcein,  $\text{CoCl}_2$  and TMRM (**A**) or calcein,  $\text{CoCl}_2$  and PI (**B,C**). After 5 min incubation ferutinin  
589 or vehicle was added to the medium. Fluorescence values were obtained by averaging pixel  
590 intensities after background subtraction and were normalised as a percentage of the maximal  
591 value. Each trace represents the mean  $\pm$  SEM of four to seven experiments.

592

593 **Figure 3:** Effect of CypD deletion and cyclosporine A on ferutinin-induced mitochondrial  
594 calcein loss and propidium iodide fluorescence increase in mouse cardiomyocytes.

595 **A and B:** Time course of calcein (**A**) and propidium iodide (PI) fluorescence (**B**) in WT and  
596 CypD-KO mouse cardiomyocytes after ferutinin exposure (arrow; 25  $\mu\text{M}$ ). Each trace  
597 represents the mean  $\pm$  SEM of six experiments.

598 **C:** CypD deletion and cyclosporine A did not prevent the effect of 12.5  $\mu\text{M}$  ferutinin on calcein  
599 loss and PI fluorescence increase. Each trace represents the mean  $\pm$ SEM of four to six  
600 independent experiments and the corresponding mean times for loss of calcein and cell death  
601 are shown in **D**.

602

603 **Figure 4:** Ferutinin induces mitochondrial swelling in isolated mouse cardiac mitochondria.

604 **A:** representative experiments and corresponding bar graphs showing swelling assessed by  
605 measuring the absorbance of the mitochondrial suspension at 540 nm. Mitochondria (0.2  
606 mg/mL (red curves) and 0.4 mg/mL (blue curves) were incubated in the respiration buffer  
607 including 5 mM glutamate/malate and increasing concentrations of ferutinin (arrow) were  
608 added at 40 s. Curves are representative of at least four independent experiments.

609 **B:** representative experiments and corresponding bar graphs showing swelling assessed as  
610 in (A) with mitochondria (0.2 mg/ml). When used cyclosporine A (CsA, 1 $\mu\text{M}$ ) was  
611 introduced at the beginning of the experiment. \* $p < 0.05$  vs 25  $\mu\text{M}$ ; #  $p < 0.05$  vs 50  $\mu\text{M}$ .  
612 Curves are representative of at least four independent experiments.

613 **C:** representative experiments and corresponding bar graphs comparing mitochondrial  
614 swelling in the respiration (RB) or in a sucrose-hepes buffer (SHB). Mitochondria (0.2  
615 mg/mL) were incubated in the respiration buffer (RB) or in a sucrose-hepes buffer  
616 (SHB) in the presence of rotenone (1 $\mu\text{M}$ ) and antimycin (1  $\mu\text{M}$ ) in order to inhibit  
617 respiration. Ferutinin (50  $\mu\text{M}$ ) was added at 40 s. When used CsA (1 $\mu\text{M}$ ) was  
618 introduced at the beginning of the experiment. \* $p < 0.05$  versus RB.

619 Curves are representative of at least four independent experiments.

620

621 **Figure 5:** Effect of ferutinin on mitochondrial oxygen consumption and membrane potential in  
622 isolated mouse heart.

623 **A:** Ferutinin inhibits mitochondrial oxygen consumption in a concentration-dependent  
624 manner. State 3 (V3) and state 4 (V4) respiration rates were measured. V4 was evaluated  
625 either after exhaustion of ADP (V4) or after addition of 1  $\mu\text{M}$  of carboxyatractyloside (CAT;  
626  $V4_{\text{CAT}}$ ) and the corresponding respiratory control ratios (RCR and  $\text{RCR}_{\text{CAT}}$ ) were evaluated.  
627 Each value represents the mean  $\pm$  S.E.M. of at least four independent experiments.  $p < 0.05$   
628 versus 0  $\mu\text{M}$  ferutinin value for V3 (§), V4(\*),  $V4_{\text{CAT}}$ (†), RCR (+) and  $\text{RCR}_{\text{CAT}}$  (#).

629 **B:** Typical experiment and corresponding bar graph showing the effect of  
630 carboxyatractyloside (CAT) on the substrate-dependent respiration rate induced by ferutinin.  
631 Oxygen consumption was induced by glutamate/malate. Addition of ferutinin (25  $\mu\text{M}$ )

632 stimulates oxygen consumption which was reversed by addition of CAT (1  $\mu$ M). Oxygen  
633 consumption rates (nmol/mL/min) are indicated in parentheses next to the curve.

634 Bar graph: Each value represents the mean  $\pm$  SEM of at least six independent preparations.

635 \* $p < 0.05$  versus basal;  $^{\S} P < 0.05$  versus respective ferutinin value.

636 **C:** Representative experiment and corresponding bar graph showing changes in  
637 mitochondrial membrane potential ( $\psi_m$ ) recorded over time by measuring the uptake/release  
638 of the fluorescent dye rhodamine 123. Increasing concentrations of ferutinin (6.25, 12.5,  
639 17.5, 25 and 50  $\mu$ M) were added at 140 s. FCCP (1  $\mu$ M) was used for comparison. Control,  
640 no addition. Curves are representative of at least four independent experiments. Bar graphs  
641 represent changes in fluorescence between 100 and 200 s. \* $p < 0.05$  versus FCCP value.

642 **D:** Typical experiment and corresponding bar graph showing the effect of  
643 carboxyatractyloside (CAT) on the decrease in membrane potential induced by ferutinin.  
644 Bar graph represents changes in fluorescence between the addition of FCCP or ferutinin and  
645 the end of the experiment (200 s). Each value represents the mean  $\pm$  SEM of at least six  
646 independent preparations.

647 \* $p < 0.05$  versus respective ferutinin value.

648

649 **Figure 6:** Ferutinin modulates mitochondrial matrix alkalinization

650 **A:** Mitochondrial pH<sub>i</sub> was studied by following BCECF fluorescence. Mitochondria were  
651 incubated in the respiration buffer until signal stabilization. Curve a: the addition of  
652 glutamate/malate (G/M) at 50 s generated membrane potential, thus matrix alkalinization.  
653 Addition of FCCP decreased pH<sub>i</sub>. Curve b: the addition of 1  $\mu$ M rotenone from the beginning  
654 of the experiment inhibited the effects of G/M and FCCP.

655 **B:** Effect of increasing concentrations of ferutinin on pH<sub>i</sub>. Experimental conditions were  
656 similar to **A** and FCCP (1  $\mu$ M) or ferutinin (6.25, 12.5, 25 and 50  $\mu$ M) were added at 250 s.

657 **C:** Effect of increasing concentrations of ferutinin on pH<sub>i</sub> in deenergized conditions.  
658 Mitochondria were incubated in the respiration buffer in the presence of rotenone and  
659 antimycin. After 40 s increasing concentrations of ferutinin (12.5, 25 and 50  $\mu$ M) were added.  
660 0: no ferutinin addition.

661 **D:** comparison of the effect of 50  $\mu$ M ferutinin on pH<sub>i</sub> in the respiration (RB) and the sucrose-  
662 Hepes (SHR) buffers supplemented or not with NaCl 100mM, KCl 100mM or cyclosporine A  
663 (CsA) 1  $\mu$ M.

664 **Figure 7:** Effect of ferutinin on mitochondrial potassium flux. Mitochondrial potassium was  
665 studied by following PBFI fluorescence.

666 **A:** Representative experiment showing the effect of increasing concentrations of ferutinin  
667 (12.5 and 25  $\mu\text{M}$  (added at 75 s) and 50  $\mu\text{M}$  (added at 100s)) after energization of  
668 mitochondria by addition of glutamate/malate (G/M). 0: no addition.

669 Curves are representative of at least four independent experiments.

670 **B:** Representative experiment and corresponding bar graph showing the effect of ferutinin in  
671 deenergized conditions (without addition of substrate and in the presence of rotenone +  
672 antimycin). After 40 s of stabilization, increasing concentrations of ferutinin (6.25, 12.5, 25,  
673 37.5, 50  $\mu\text{M}$  and 50  $\mu\text{M}$  ferutinin + 1 $\mu\text{M}$  cyclosporine A (CsA)) were added. CsA was added  
674 at the beginning of the experiment. Curves are representative of at least four independent  
675 experiments. Bar graph represents changes in fluorescence between 30 and 150 s. \* $p < 0.05$   
676 vs control.

677

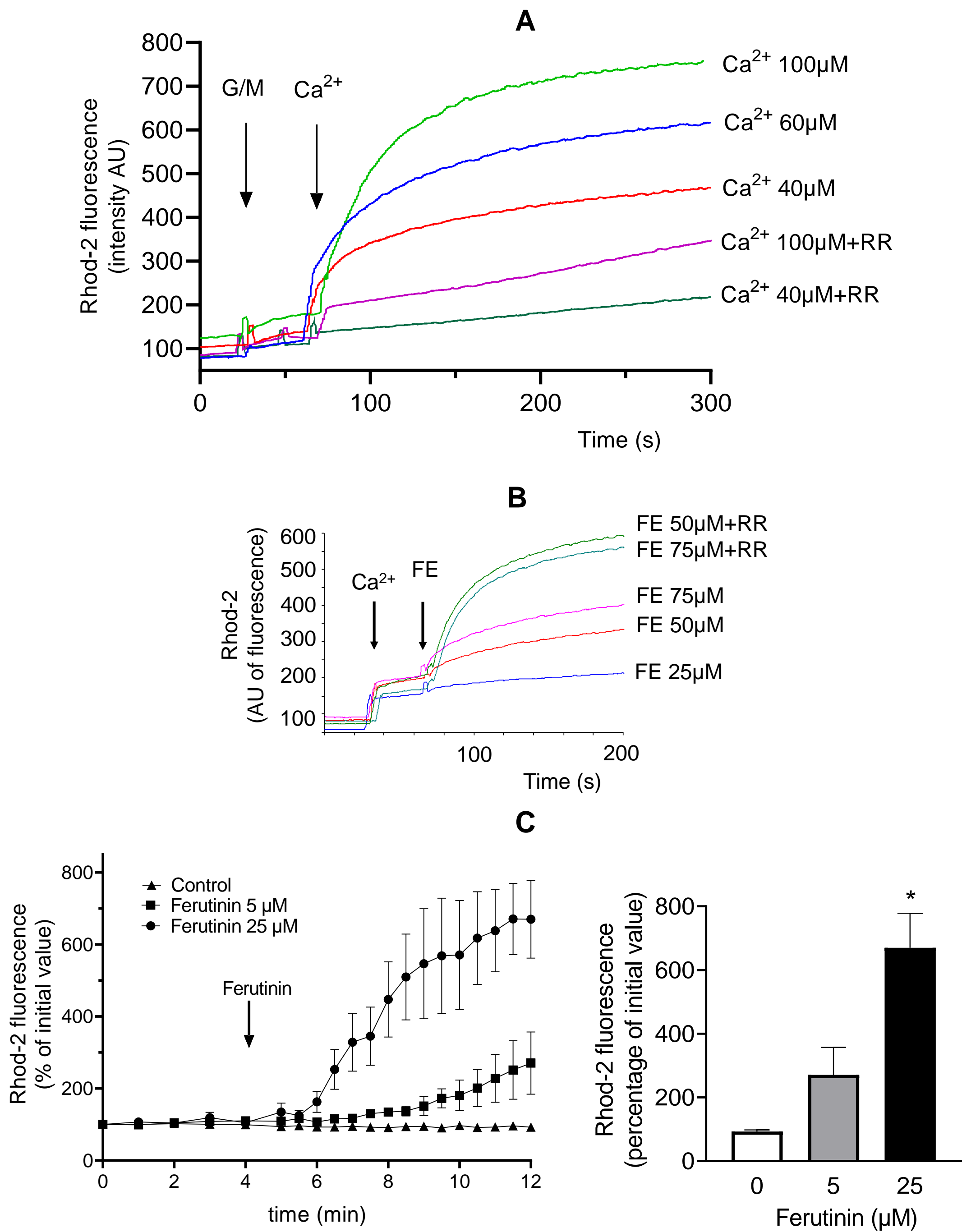


Fig 1

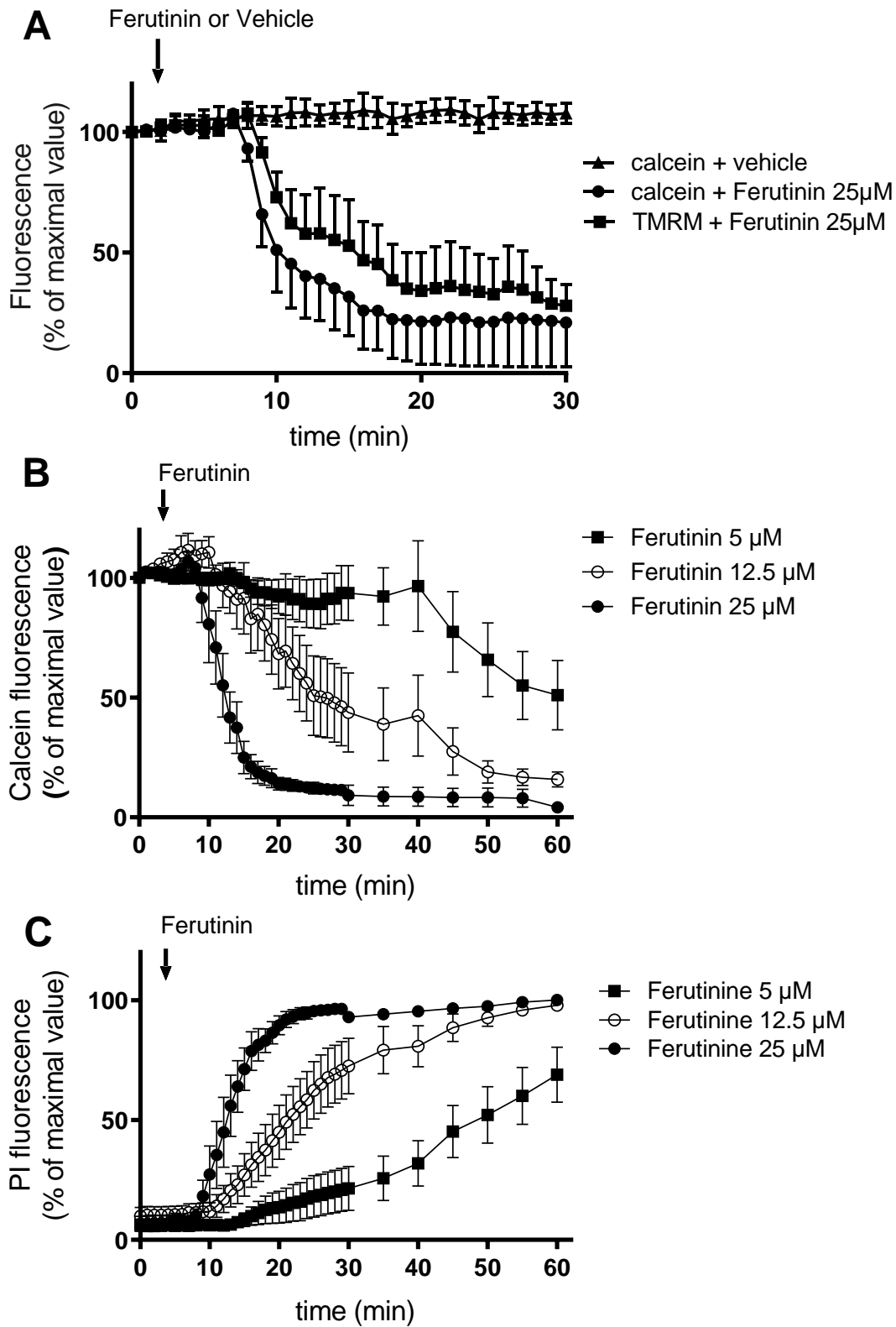
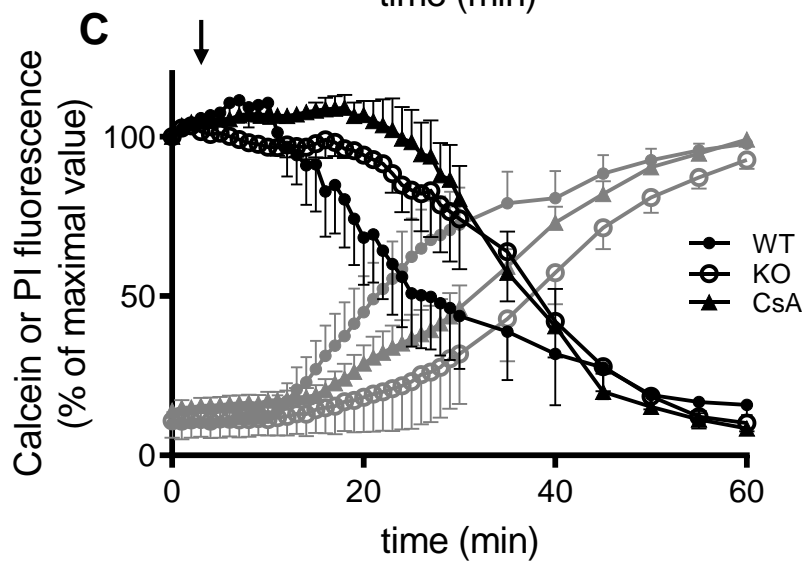
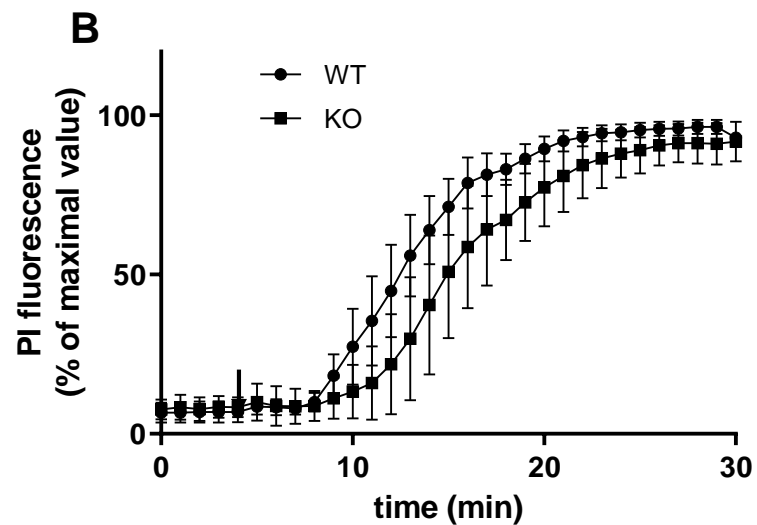
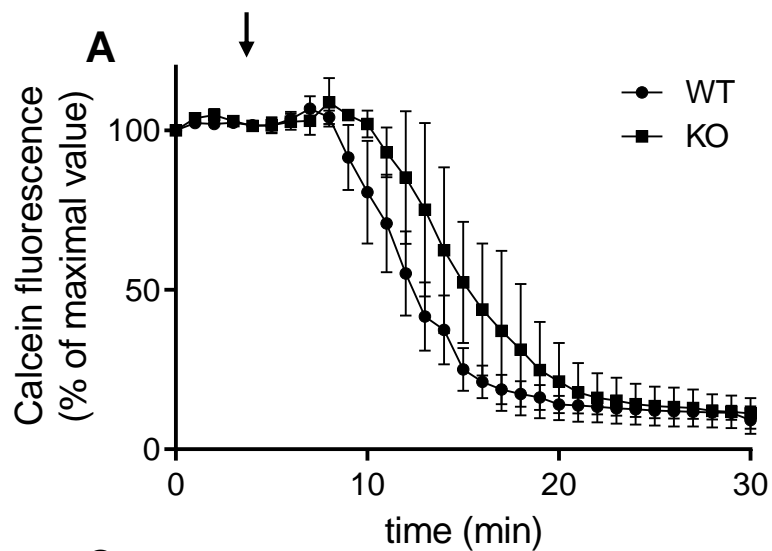


Fig 2



**D**

	$T_{\text{calcein50}}$ (min)	$T_{\text{celldeath50}}$ (min)
Control	$25.4 \pm 4.30$	$24.8 \pm 3.5$
CsA	$33.6 \pm 2.25$	$32.0 \pm 3.0$
Cyp-D KO	$35.9 \pm 4.02$	$36.7 \pm 6.0$

Fig 3

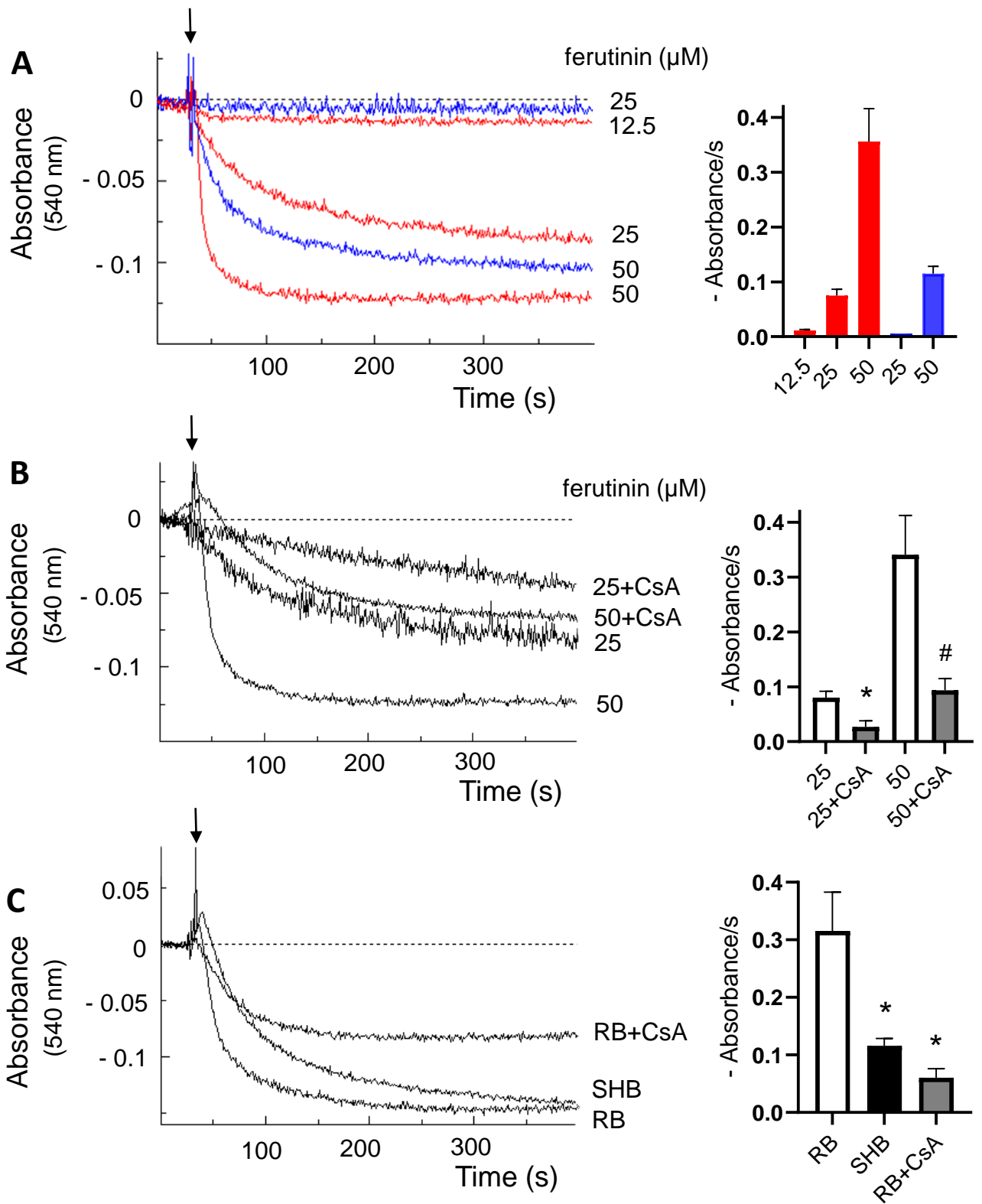


Fig 4

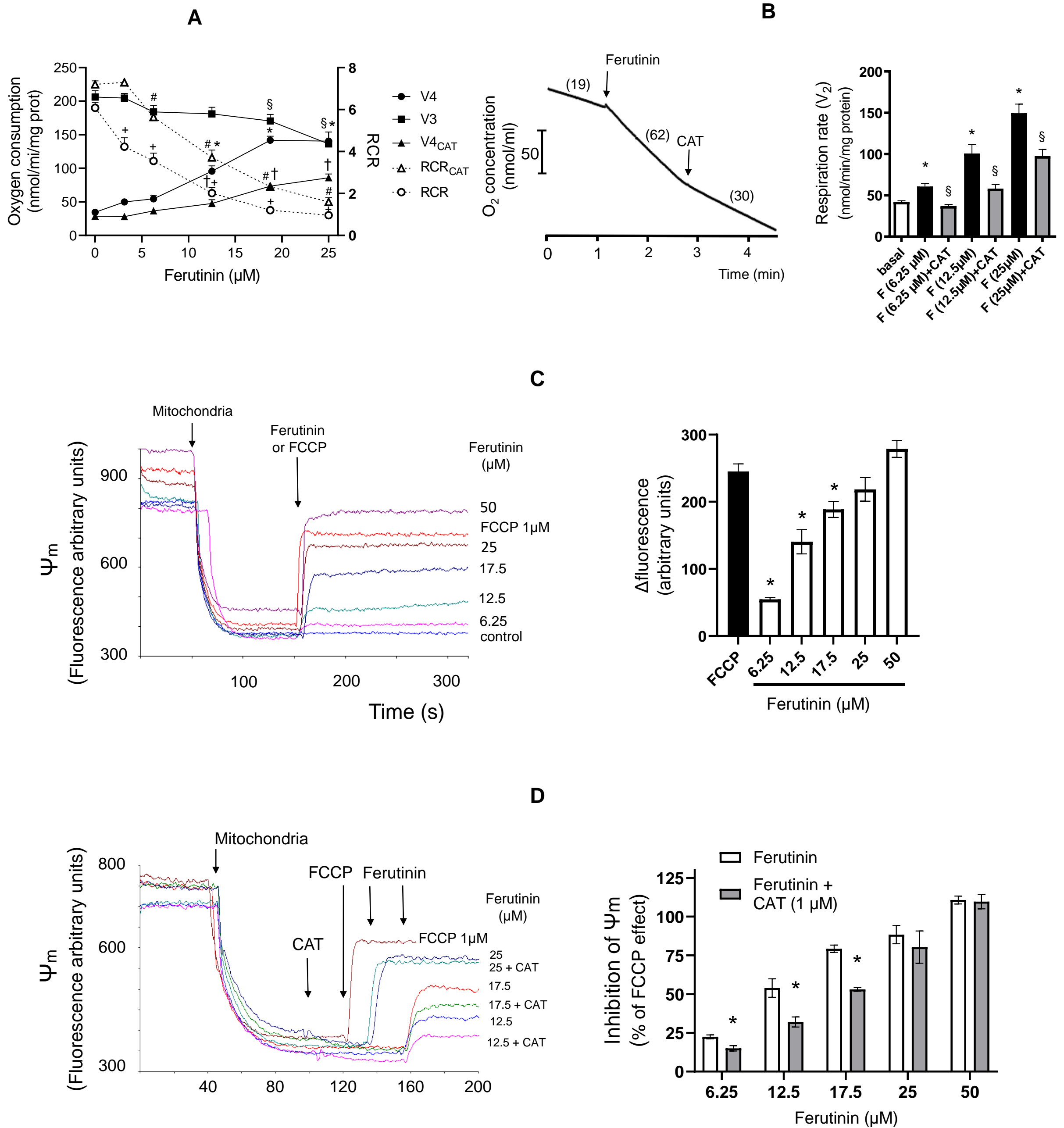


Fig 5

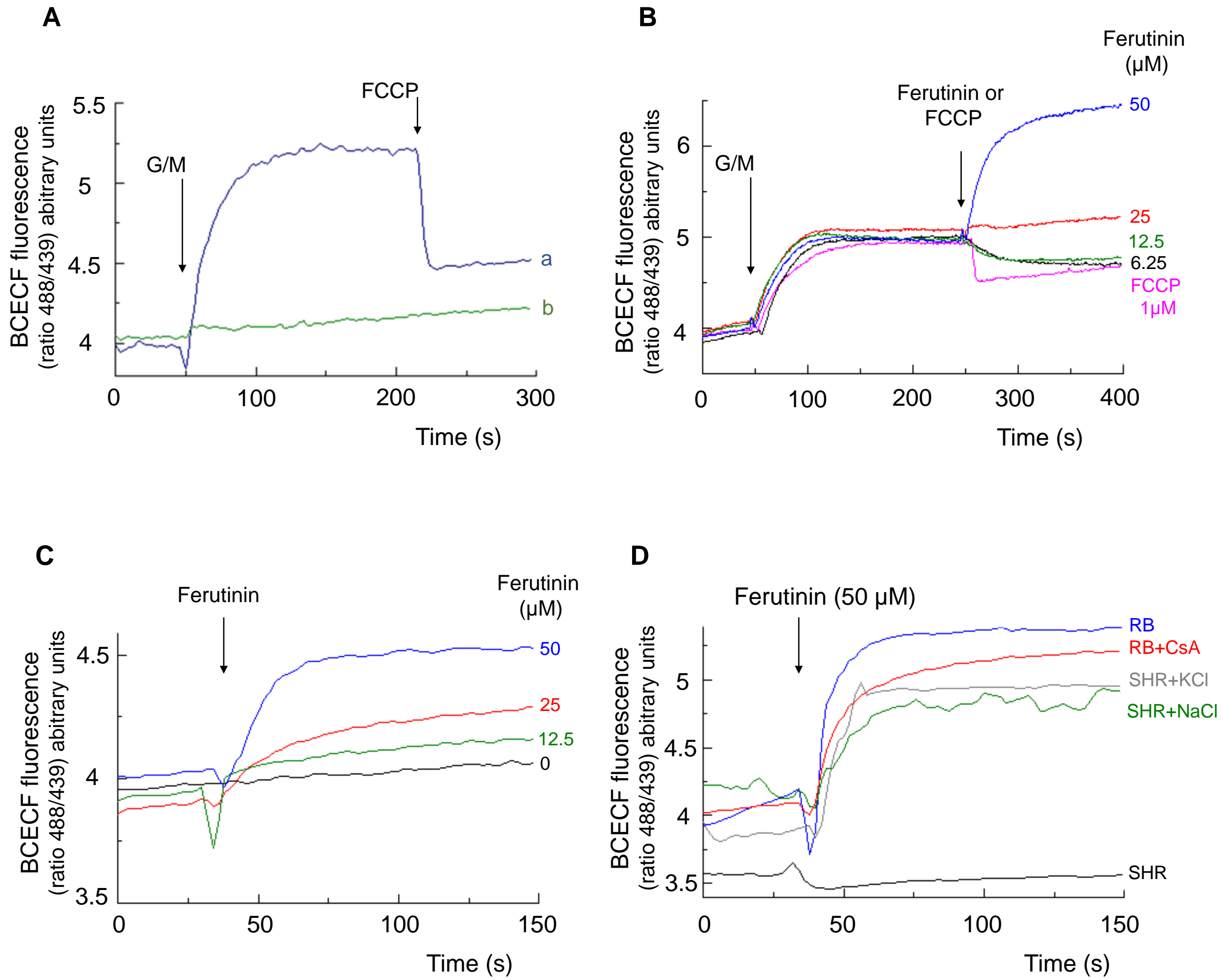


Fig 6

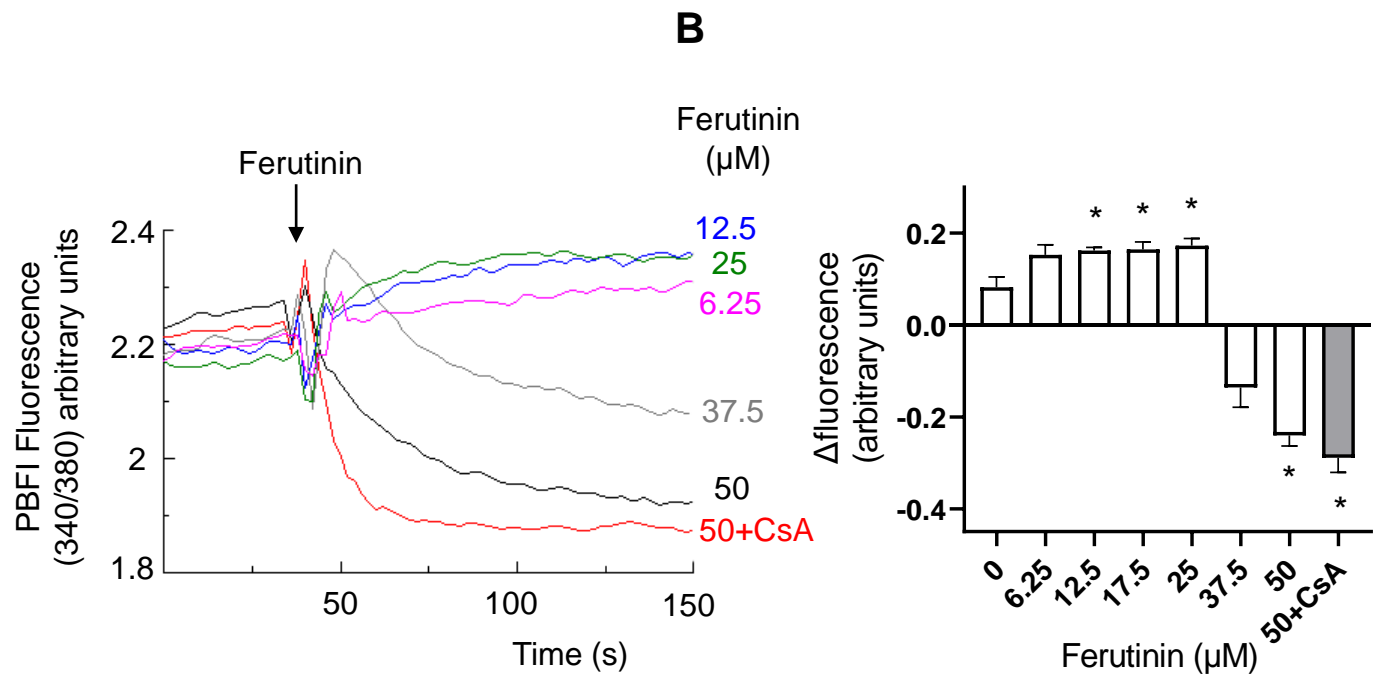
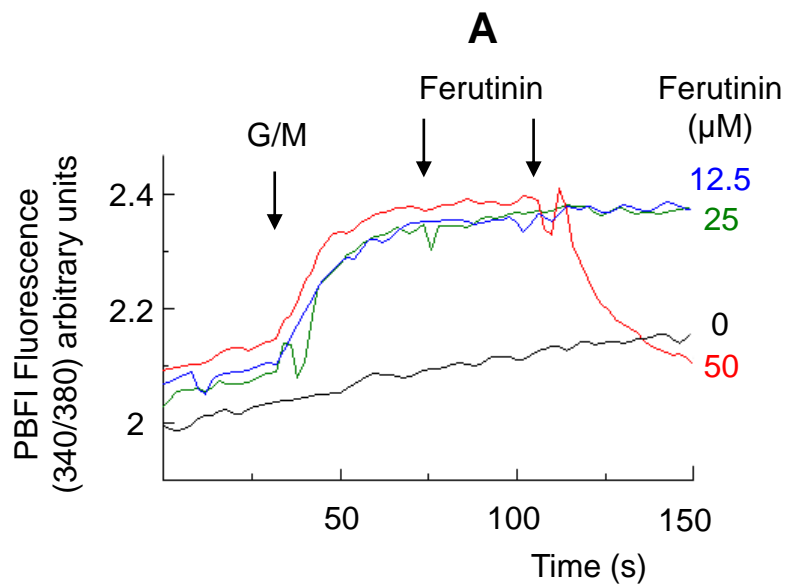


Fig 7

## Supplementary material

### Opening of mitochondrial permeability transition pore in cardiomyocytes: is ferutinin a suitable tool for its assessment?

Juliette Bréhat, Mathieu Panel, Bijan Ghaleh, Didier Morin

INSERM U955-IMRB, team Ghaleh, UPEC, Ecole Nationale Vétérinaire d'Alfort, Créteil,  
France.

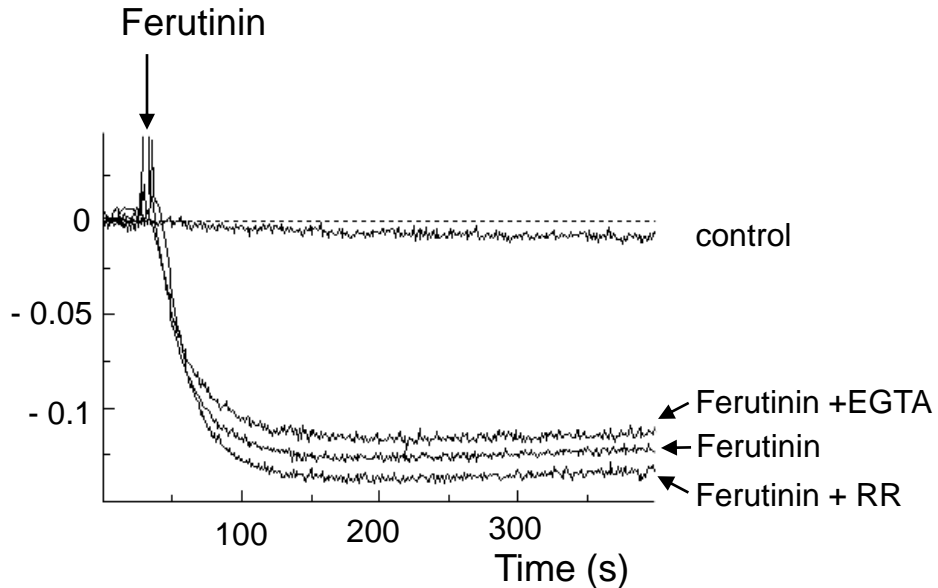


**Figure S1.**

Ferutinin induces mitochondrial swelling is not inhibited by EGTA and ruthenium red in isolated mouse cardiac mitochondria. Swelling was assessed by measuring the absorbance of the mitochondrial suspension at 540 nm. Mitochondria (0.2 mg/mL) were incubated in the respiration buffer in the presence of rotenone (1  $\mu$ M) and antimycin (1  $\mu$ M). Ferutinin (50  $\mu$ M) was added at 40 s. When used, EGTA (100  $\mu$ M) and ruthenium red (RR, 5  $\mu$ M) were introduced at the beginning of the experiment. Control: no addition of ferutinin. Curves are representative of at least four independent experiments.

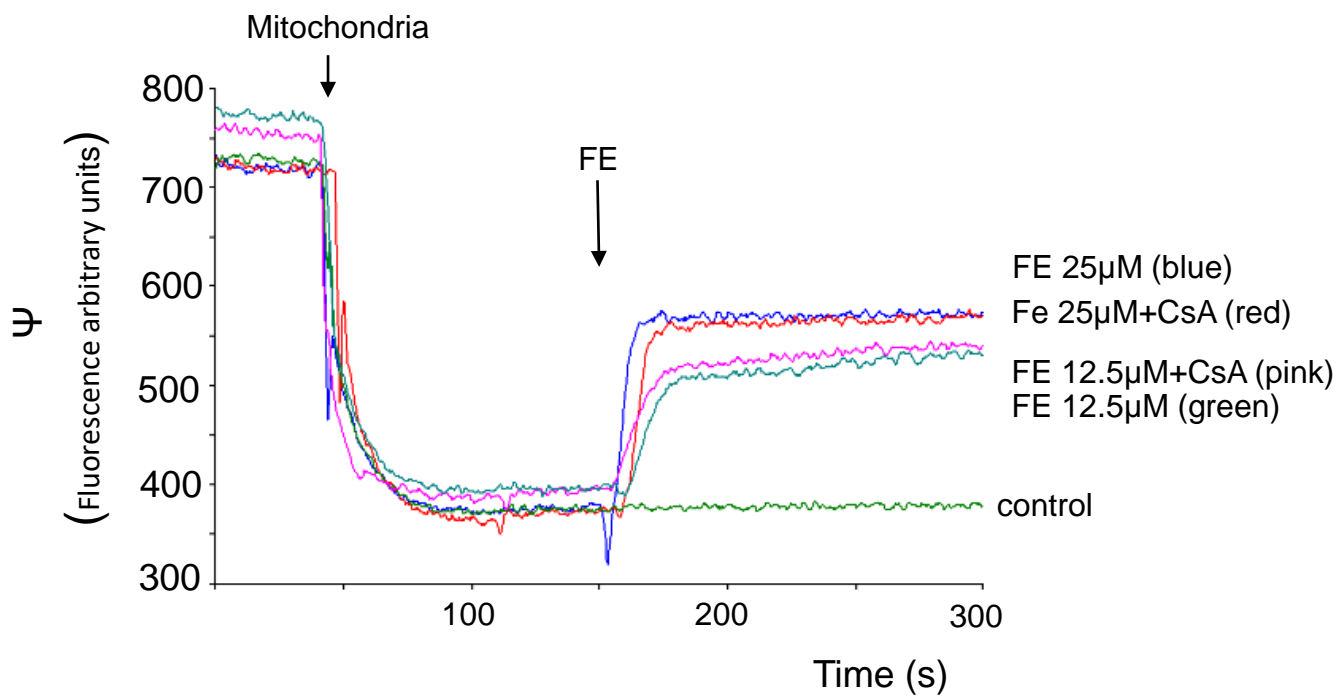


**Figure S2.**

Representative experiment showing the lack of effect of cyclosporine A on the decrease in membrane potential induced by ferutinin. Changes in membrane potential ( $\psi$ ) was recorded over time by measuring the uptake/release of the fluorescent dye rhodamine 123. Cyclosporine A (CsA, 1  $\mu$ M) was added at the beginning of the experiment and ferutinin (FE, 12.5 and 25  $\mu$ M) at 140 s. Control: no addition. Curves are representative of at least four independent experiments.